COMPUTED TOMOGRAPHIC APPEARANCE OF MELANOMAS IN THE EQUINE HEAD: 13 CASES

Jonathon Dixon[1], Ken Smith[1], Justin Perkins[1], Ceri Sherlock[2], Tim Mair[2], Renate Weller[1]

[1] Department of Clinical Sciences and Services, The Royal Veterinary College, Hawkshead Lane, Hatfield, AL9 7TA

[2] Bell Equine Veterinary Clinic, Butchers Lane, Mereworth, Kent, ME18 5GS

Key words: Computed Tomography, Equine, Melanoma, Neoplasia

Running Head: CT appearance of equine melanomas

Funding Sources: None

Corresponding author: rweller@rvc.ac.uk

Abstract

Melanomas are one of the most common neoplasms in the horse and are frequently found in the head region. There is a genetic predisposition in horses with a grey hair coat. Computed tomography (CT) is frequently used in referral practice to evaluate the equine head but there are few reports describing the CT appearance of melanomas in this location. The aim of this study was to describe a retrospective, descriptive, case series of horses with this condition. Case records from two referral hospitals were reviewed, and thirteen horses were identified that had undergone CT of the head, with a diagnosis of melanoma based on cytology, histopathology or visual assessment of black (melanotic) tissue. A median of 11 melanomas was identified per horse (range 3-60), with a total of 216 masses. Melanomas were found most frequently in the parotid salivary gland, guttural pouches, surrounding the larynx and pharynx and adjacent to the hyoid apparatus. In non-contrast CT images, all melanomas were hyperattenuating (median; 113.5 Hounsfield units (HU), IQR; 26 HU) compared to masseter musculature (median; 69 HU, IQR; 5.5 HU). Fifty-six (25.9%) masses were partially mineralized and forty-one (19.4%) included hypoattenuating areas. Histopathological assessment of these melanomas suggests that the hyperattenuation identified is most likely a result of abundant intracytoplasmic melanin pigment. Melanomas of the equine head appear to have consistent features on CT, which aids diagnosis of mass lesions and their distribution in this area, although histopathological analysis or visual confirmation should still be obtained for definitive diagnosis.

Introduction

Melanomas are one of the most frequently identified neoplasms in horses, representing between 3 and 15% of tumours, with a known genetic predisposition identified in the grey horse.[1] Melanomas are frequently identified in the perineal region, the base of the tail, the lips and the prepuce.[1-3] However they have also been frequently reported to affect the head and neck.[4-6]

In the head, melanomas have been described affecting the parotid salivary glands, eye and eyelids, ears, guttural pouches, paranasal sinuses, lymph nodes and other cutaneous sites.[1, 5, 7-11] While some of these are visible on clinical examination, some affect deeper structures which may only be identified via endoscopy of the guttural pouches, computed tomography (CT) or magnetic resonance (MR) imaging. There are several publications that describe the use of CT for the evaluation of mass lesions in the head.[12-14]

Equine melanomas vary from being heavily pigmented to non-pigmented (amelanotic). Most melanomas are pigmented and the dark brown to black appearance of these masses is a result of abundant intracellular melanin pigment.[1] Melanin is formed from the oxidation and subsequent polymerization of the amino acid L-tyrosine which occurs within the melanocytes.[15] Melanin has been noted to exhibit paramagnetic effects in MR images of both humans and small animals.[16-20]

Many different neoplasms and mass like lesions have been reported to affect the equine head, including but not limited to; adenocarcinoma, lymphosarcoma, haemangiosarcoma, squamous cell carcinoma, osteosarcoma, myxoma, meningioma, ossifying fibroma, anaplastic sarcoma, spindle cell tumour progressive ethmoidal haematoma and melanoma.[5, 11, 13, 21-25] In one CT study, all

sinonasal neoplasms with the exception of the ossifying fibroma, were identified to be iso- or hypoattenuating when compared to the masseter muscle.[13] In another study, progressive ethmoidal haematomas were noted to be hyperattenuating compared with masseter muscle and the hyperattenuation was described most commonly as heterogeneous with a 'swirling' pattern.[16] Computed tomography attenuation values alone do not differentiate between various neoplasms, normal soft tissue structure or even purulent material.[13] However, there are two cases within the reported literature describing CT imaging findings in horses with melanoma, both of which demonstrated the presence of a hyperattenuating mass.[10, 21]

The authors have identified melanomas in the head of horses using CT and these masses were observed to be hyperattenuating to surrounding musculature, often with a mineralized component. Our clinical experience matches case reports in the human literature describing the CT features of melanoma in the head, in particular the brain; frequently melanoma masses are hyperattenuating compared to both brain parenchyma and adjacent musculature.[26, 27]

The aim of the present study was to describe the CT imaging features of melanomas in the horse. The hypothesis is that melanomas will be consistently hyperattenuating to surrounding masseter musculature on CT images.

Methods

Cases records of horses that had standing CT at the Equine Referral Hospital, The Royal Veterinary College (RVC) between April 2010 until April 2015 and at Bell Equine Veterinary Clinic (BEVC) between April 2013 and April 2015 were reviewed. Cases were only included if they had at least one mass lesion identified

on standing CT that was diagnosed as melanoma on the basis of cytological examination of a fine needle aspirate, histopathological evaluation of an incisional or excisional biopsy, or visual assessment of black tissue representing the mass e.g. within the guttural pouch on endoscopy. The case history, signalement, primary presenting complaint and clinical findings of all horses included in this study were reviewed from the hospital records system, and summarized for this study. Cases where either a complete CT studies or a definitive diagnosis were not available were excluded from this study.

CT images were reviewed jointly by two authors, one ECVDI LA Associate (RW) and one ECVDI LA track resident (JD) in a single sitting using a computer workstation and DICOM viewing software (OsiriX 64 bit version 6.0.2, Pixmeo SARL, Switzerland). Reviewers utilized multiplanar reconstructions (MPR) and adjustments of the window width (WW) and window level (WL).

Reviewers recorded the number of masses identified, the anatomical location of masses, the maximum mass dimensions, representative mean tissue attenuation of each mass (Hounsfield unit, (HU)), comparative mean attenuation of the masseter muscle, presence and attenuation values of hypoattenuating regions within a mass, and the presence and attenuation values of any mineralization within a mass. Representative attenuation values were obtained for each of the variety of regions using the maximum possible round or oval shaped, hand drawn region of interest (ROI) on a transverse image of each respective lesion. Due to the variable size of lesions, ROI size could not be standardized. All CT studies were reviewed by both the first and last authors to identify signs of concurrent pathology. Abnormalities were recorded and significance determined by presenting signs and the clinical experience of the reviewers.

Histopathological reports and retained specimens were retrospectively reviewed by a board certified veterinary pathologist (KS).

Data distribution was assessed by evaluating histograms; a Wilcoxon Signed Rank test was consequently performed to assess the difference in Hounsfield units between masses and the masseter muscle. P-values were set at 0.05 and analysis was performed in SPSS (IBM SPSS Statistics, version 21.0, IBM Corp, Armonk, NY, USA). Analysis of data was performed by the first and last authors.

Results

Thirteen horses met the inclusion criteria for this study (7 from The RVC, and 6 from BEVC). Breeds were 6 Irish Sports Horses, 2 Irish Draft Horses, 2 Connemaras, 1 Thoroughbred, 1 Arabian cross and 1 pony. There were 4 geldings and 9 mares. Median age was 12 years (range 6-24 years). All horses had a grey hair coat.

Computed tomographic images were obtained in the standing, sedated horse as has been previously described,[28] using one of two multidetector CT scanners (RVC: GE LightSpeed Pro 16, GE Healthcare, Buckinghamshire, UK and BEVC: GE LightSpeed Plus, GE Healthcare, Buckinghamshire, UK), with typical scan parameters of 1.25mm thick slices, 1.25mm interslice gap, tube rotation time of 0.5-0.8 seconds, kVp of 120 and mA of 200 and a variable pitch. CT scans were typically performed from the junction between the first and second cervical vertebrae rostrally to include the entire dental arcades to the level of the diastema. Non-ionic iodinated contrast media (Iohexol, 300mg/ml, Omnipaque, GE Healthcare, UK) was administered in a single case at a dose of 300mgI/kg IV using hand administration through bilateral 12 gauge jugular catheters followed

by repeated image acquisition at both 30 seconds and 90 seconds post injection. Image reconstruction using both soft tissue and bone algorithms was routinely performed.

The primary presenting signs were; soft tissue swelling in the parotid salivary gland region in 6 horses, dysphagia in 3, and mass at the base of the ear, exophthalmos, mass over the temporomandibular joint and unilateral nasal discharge each affecting one horse. One of the CT examinations was performed as part of a pre-purchase examination due to the detection of mass lesions in the parotid salivary gland region on clinical examination.

Diagnosis of melanoma was based on sampling a sub-section of masses (1-2 per horse) using histopathology in 6 horses, cytology in 2 and visualization of a black mass within one or both guttural pouches in 5.

A total of 216 soft tissue masses compatible with melanoma were identified in the 13 horses (median 11; range 3-60). The location of the melanomas detected in these cases are detailed in Table 1, with melanomas identified most frequently in the region of the parotid salivary gland, guttural pouches, surrounding the larynx and pharynx and adjacent to the hyoid apparatus. There was a wide variability in the size of melanomas (identified on transverse CT images) with the smallest identified being 3 x 3mm and the largest 136 x 104mm in the transverse plane. Example images are given in Figure 1 A-D.

Masses generally appeared as well demarcated homogenous areas of hyperattenuation compared with adjacent soft tissue, with some containing hypoattenuating or mineral attenuating areas. Median representative attenuation of the 216 masses was 113.5 HU (IQR; 26 HU). Median attenuation of masseter muscle measured was 69 HU (IQR; 5.5 HU). When compared to each

individual horses' masseter musculature, all 216 of the identifiable melanoma masses were observed to be hyperattenuating. There was a significant difference in attenuation values between the melanoma masses and the masseter muscle (P=0.01).

Irregularly shaped but well-defined hypoattenuating regions were identified within 19.4% (41/216) of the individual masses. The median attenuation of these hypoattenuating regions was 45.1 HU (IQR; 29.5 HU). Of the 216 total masses identified, 25.9% (56/216) were found to have mineral content within the mass, with a median attenuation of 326 HU (IQR; 163.75 HU).

Concurrent abnormalities were identified in CT images of 6 horses. The most frequently identified concurrent abnormalities included; two cases with periapical infection of a cheek tooth (teeth 109 and 209), one of which had a secondary sinusitis, two cases with temporohyoid articulation remodeling and two cases with osteophytes affecting the temporomandibular joints. In 11/13 cases the melanomas were considered the primary clinical problem, and the reason for performing advanced imaging. In the two cases where melanomas were not the primary clinical complaint, one case had dental disease and secondary sinusitis, and one case presented for a laryngeal foreign body (metal wire). The use of CT in each of these cases facilitated a greater understanding of the number and extent of masses within the head region, often identifying a significantly greater number of lesions than clinical examination alone revealed.

Post contrast CT images were obtained in one horse with a parotid melanoma. This enabled detailed assessment of the local vasculature, which aided in surgical planning. In this case, the masses showed moderate and relatively homogenous

enhancement following contrast administration (72HU pre-contrast, 110HU post contrast).

Histopathological evaluation

Specimens of melanomas from 3 horses were available for histological review. On histological examination the typical appearance was that of an expansile to infiltrative unencapsulated mass composed of small nests and short interwoven bundles of polygonal to spindle-shaped cells with fine intracytoplasmic melanin granules (neoplastic melanocytes) interspersed with aggregates of large round cells containing abundant coarsely granular intracytoplasmic melanin (melanomacrophages). The neoplastic melanocytes demonstrated mild nuclear atypia and scattered mitoses: average less than 1 per 10 high power field (Figure 2). Intralesional haemorrhage was rare. Some sections contained irregular areas of ischaemic-type necrosis that was undergoing mineralization (dystrophic calcification).

Discussion

A median of 11 melanoma mass lesions were identified on CT images acquired standing in 13 horses. All masses showed a similar consistent appearance on CT images, appearing as a well-defined, predominantly homogenous mass lesion (median attenuation of 113.5 HU) that was hyperattenuating compared with masseter musculature (median attenuation of 69 HU). This finding suggests a means to distinguish melanomas from the surrounding normal musculature; hence measurement of the attenuation value should be included when reviewing CT images of horses with suspected melanoma.

Melanomas are one of the most frequently identified neoplasms in the horse.[1] Despite a large clinical CT caseload at the two hospitals in this study, there were only 13 cases presented for computed tomographic evaluation with subsequent lesion confirmation over the study period. It is likely that the low number of horses identified with melanomas on CT is a result of lesions being identified and treated within first opinion practice and the potential advantages of CT being under-recognized.

In humans the hyperattenuating appearance of melanoma on CT has been associated with intra-tumoural hemorrhage,[26] however this was rarely found on histopathological review of tissue sections in the present study. Hemorrhage on CT can often be visualised as a hyperattenuating lesion due to the degree of cellularity and subsequent breakdown products of a hematoma and therefore is an important factor to consider.[29, 30] In the absence of significant intralesional haemorrhage we instead propose that the hyperattenuating appearance in the lesions that we imaged to directly reflect the melanin content.[18, 31] Melanin pigment has been shown to have a high affinity for the binding of multiple metal ions including iron, copper, manganese and zinc, and may demonstrate free radical scavenging properties.[17] Copper is utilized in the formation of melanin pigment, being required for tyrosinase activity, and therefore may become incorporated into the molecule. It is known that melanin pigment exhibits paramagnetic effects when placed in an external magnetic field such as a clinical MR imaging scanner, and it is possible that the paramagnetic effects are also a direct result of this high metal ion binding affinity.[16] The relatively high atomic number of these metal ions explains the relatively high attenuation of melanin-

containing melanomas in CT images. The melanomas identified in the present study were melanin-containing (melanotic) melanomas.

In one horse in the present series, which had 4 masses, attenuation values of the melanoma lesions were in the range of 69-77HU. Although still hyperattenuating compared to the masseter muscle in this individual (67HU), these values were lower than those of the other twelve horses. The melanomas in this individual were small and poorly delineated from the surrounding parotid salivary gland parenchyma, hence the measured attenuation values may underestimate the true attenuation because of partial volume effects. The authors chose to include this case despite these challenges, as the subtlety of the masses identified represents a real-life clinical problem that must be recognized when evaluating for the presence of lesions on CT images.

Mineralization of the melanoma masses was observed commonly in this series (25.9% of masses), with this often seen in association with adjacent hypoattenuating regions. This corresponds to the histological finding of melanomas with areas of necrosis adjacent to secondary areas of dystrophic mineralization. This secondary change is rarely observed in melanomas in other species.[32-35]

Post-contrast CT of standing horses is not a widely established technique and was used for only one horse in this series therefore the potential benefit of acquiring post-contrast images cannot be assessed on the basis of a single case.

The results of this study suggest that melanomas are readily visible on non-contrast CT images when the CT images are viewed on an appropriate WW and WL. This point reinforces the importance of using both a bone (WW; 3000, WL;

700) and a soft tissue (WW; 350, WL; 50) window when evaluating the head of the horse.

It is beyond the scope of this article to review in depth the treatment options for melanomas of the head and this information is largely available elsewhere.[1] A range of treatment options was utilized in the patients within this study, and this reflects clinician preferences, lesion location, the number and extent of the lesions, the clinical consequences of the lesions and use of the horse. In some cases, a greater number of masses were identified on the CT images than were clinically suspected, with 60 masses identified in one patient. It therefore seems appropriate to consider that some superficial lesions identified on clinical examination may well represent only 'the tip of the iceberg' in regards to the true number of masses present and diagnostic imaging is recommended to enable individual equine patients to be accurately staged to permit informed decision making about case management.

When examining lesions of this nature on CT images, other differential diagnoses are that of alternative neoplasms. Several other neoplastic lesions including; osteoma, ossifying fibroma, osteosarcoma and others have been reported to contain mineral material and therefore may have a hyperattenuating appearance on CT images.[11, 13, 24] Predominantly heterogenous hyperattenuating progressive ethmoidal haematomas are less likely differential diagnoses; as, these are generally located in the sinuses or ethmoidal regions rather than within the soft tissue.[16]

With respect to limitations of this study, one challenging finding was to accurately identify each individual mass, particularly in cases where abundant masses were present in close proximity to one another. Additionally, when

291 performing attenuation measurements, rather than a using a predefined sized
292 ROI, varying sized ROI's were used in this study to evaluate the attenuation
293 values of the masses, masseter muscle and the hyper- and hypo- attenuating
294 areas within the masses. The largest ROI possible was used to reflect the
295 attenuation of the homogenous portion of the tissue of interest only, whilst
296 maximizing the sampling size in each location. Using too large a ROI may have
297 sampled perilesional tissues, and too small a ROI may not have incorporated
298 enough image information, either of which may have decreased the accuracy of
299 the measurements.[36]
300 In conclusion, melanomas in the equine head appear to have a consistent
301 appearance on CT images. This consistent appearance may aid differentiation of
302 melanomas from other soft tissue masses within the head and therefore aid
303 radiologists to identify such lesions. Melanomas in the equine head are
304 commonly numerous and appear hyperattenuating compared to masseter
305 muscle with a median attenuation of 113.5 HU. Melanomas may contain
306 hypoattenuating areas consistent with necrosis or mineral attenuating areas
307 consistent with dystrophic mineralization. Although histopathological
308 characterization of masses remains the gold standard, the authors suggest that
309 the imaging features identified may aid in forming appropriate differential
310 diagnoses when evaluating sinonasal and other head mass lesions.

Acknowledgments

The authors thank Christopher R Lamb and Tommaso Gregori for their advice and contributions to this study.

References

1. Phillips JC, Lembcke LM. Equine melanocytic tumors. *Vet Clin North Am Equine Prac*. 2013;**29**: 673-687.
2. Cotchin E. A general survey of tumours in the horse. *Equine Vet J*. 1977;**9**: 16-21.
3. Seltenhammer MH, Simhofer H, Scherzer S, Zechner P, Curik I, Solkner J, et al. Equine melanoma in a population of 296 grey Lipizzaner horses. *Equine Vet J*. 2003;**35**: 153-157.
4. McFadyean J. Equine melanomatosis. *J Comp Pathol*. 1933;**46**: 186-IN188.
5. Fintl C, Dixon PM. A review of five cases of parotid melanoma in the horse. *Equine Vet Educ*. 2001;**13**: 17-24.
6. Valentine BA. Equine melanocytic tumors: a retrospective study of 53 horses (1988 to 1991). *J Vet Intern Med*. 1995;**9**: 291-297.
7. Moore JS, Shaw C, Shaw E, Buechner-Maxwell V, Scarratt WK, Crisman M, et al. Melanoma in horses: Current perspectives. *Equine Vet Educ*. 2013;**25**: 144-151.
8. Albanese V, Newton JC, Waguespack RW. Malignant melanoma of the third eyelid in a horse. *Equine Vet Educ*. 2015;**27**: e15-e19.
9. Barnett K, Platt H. Intraocular melanomata in the horse. *Equine Vet J*. 1990;**22**: 76-82.
10. Tietje S, Becker M, Bockenhoff G. Computed tomographic evaluation of head diseases in the horse: 15 cases. *Equine Vet J*. 1996;**28**: 98-105.
11. Dixon P, Head K. Equine nasal and paranasal sinus tumours: part 2: a contribution of 28 case reports. *Vet J*. 1999;**157**: 279-294.
12. Manso-Díaz G, García-López JM, Maranda L, Taeymans O. The role of head computed tomography in equine practice. *Equine Vet Educ*. 2015;**27**: 136-145.
13. Cissell DD, Wisner ER, Textor J, Mohr FC, Scrivani PV, Theon AP. Computed tomographic appearance of equine sinonasal neoplasia. *Vet Radiol Ultrasound*. 2012;**53**: 245-251.
14. Textor JA, Puchalski SM, Affolter VK, MacDonald MH, Galuppo LD, Wisner ER. Results of computed tomography in horses with ethmoid hematoma: 16 cases (1993-2005). *J Am Vet Med Assoc*. 2012;**240**: 1338-1344.
15. Lerner AB, Fitzpatrick TB. Biochemistry of melanin formation. *Physiol Rev*. 1950;**30**: 91-126.
16. Premkumar A, Marincola F, Taubenberger J, Chow C, Venzon D, Schwartzentruber D. Metastatic melanoma: correlation of MRI characteristics and histopathology. *J Magn Reson Imaging*. 1996;**6**: 190-194.
17. Enochs WS, Petherick P, Bogdanova A, Mohr U, Weissleder R. Paramagnetic metal scavenging by melanin: MR imaging. *Radiology*. 1997;**204**: 417-423.
18. Uozumi A, Saegusa T, Ohsato K, Yamaura A. Computed tomography and magnetic resonance imaging of nonhemorrhagic, metastatic melanoma of the brain--case report. *Neurol Med Chir (Tokyo)*. 1990;**30**: 143-146.
19. Grahn BH, Stewart WA, Towner RA, Noseworthy MD. Magnetic resonance imaging of the canine and feline eye, orbit, and optic nerves and its clinical application. *Can Vet J*. 1993;**34**: 418-424.

20. Kato K, Nishimura R, Sasaki N, Matsunaga S, Mochizuki M, Nakayama H, et al. Magnetic resonance imaging of a canine eye with melanoma. *J Vet Med Sci*. 2005;**67**: 179-182.
21. Sasaki N, Minami T, Yamada K, Satoh M, Inokuma H, Kobayashi Y, et al. MDCT Images of the Head of a Horse with Malignant Melanoma. *J Equine Sci*. 2007;**18**: 55-58.
22. Dyson PK, Dunn KA, Whitwell K, Dennis R. Ataxia and cranial nerve signs in a pony suffering a brainstem meningioma; clinical, MRI, gross and histopathological findings. *Equine Vet Educ*. 2007;**19**: 173-178.
23. Silva AdC, Cassou F, Andrade B, Ramos LdO, da Paixão T, Alves G, et al. Ossifying oronasal carcinoma in a horse. *Brazilian Journal of Veterinary Pathology*. 2012;**5**: 128-132.
24. Crijns C, Vlaminck L, Verschooten F, Bergen T, De Cock H, Huylebroek F, et al. Multiple mandibular ossifying fibromas in a yearling Belgian Draught horse filly. *Equine Vet Educ*. 2015;**27**: 11-15.
25. Tremaine W. Progressive ethmoidal haematoma. *Equine Vet Educ*. 2013;**25**: 508-510.
26. Ginaldi S, Wallace S, Shalen P, Luna M, Handel S. Cranial computed tomography of malignant melanoma. *Am J Neuroradiol*. 1980;**1**: 531-535.
27. Holtås S, Cronqvist S. Cranial computed tomography of patients with malignant melanoma. *Neuroradiology*. 1981;**22**: 123-127.
28. Dakin S, Lam R, Rees E, Mumby C, West C, Weller R. Technical set‐up and radiation exposure for standing computed tomography of the equine head. *Equine Vet Educ*. 2014;**26**: 208-215.
29. Bradley WG, Jr. MR appearance of hemorrhage in the brain. *Radiology*. 1993;**189**: 15-26.
30. Parizel PM, Makkat S, Van Miert E, Van Goethem JW, van den Hauwe L, De Schepper AM. Intracranial hemorrhage: principles of CT and MRI interpretation. *Eur Radiol*. 2001;**11**: 1770-1783.
31. Kalkman E, Baxter G. Melanoma. *Clin Radiol*. 2004;**59**: 313-326.
32. Chénier S, Doré M. Oral malignant melanoma with osteoid formation in a dog. *Veterinary Pathology Online*. 1999;**36**: 74-76.
33. Pellegrini AE, Scalamogna PA. Malignant melanoma with osteoid formation. *Am J Dermatopathol*. 1990;**12**: 607-611.
34. Lucas DR, Tazelaar HD, Unni KK, Wold LE, Okada K, Dimarzio Jr DJ, et al. Osteogenic melanoma: a rare variant of malignant melanoma. *Am J Surg Pathol*. 1993;**17**: 400-409.
35. Fukunaga M. Osteogenic melanoma. *Apmis*. 2005;**113**: 296-300.
36. Wörz S, Rohr K. Localization of anatomical point landmarks in 3D medical images by fitting 3D parametric intensity models. *Medical Image Analysis*. 2006;**10**: 41-58.

Tables

Table 1: Summary of signalement, presenting complaints and melanoma measurements obtained from 13 horses.

Case	Age in years	Breed	Sex	Presenting complaint	Lesion locations	Number of masses identified	Median attenuation of masses (HU)	Maximum mass dimension in the transverse plane (mm)	Mineralization of masses present (Y/N)	Hypoattenuating areas present (Y/N)
1	12	Pony	FE	Parotid soft tissue swelling	PX, LX, GP, EA, TMJ	32	109	136 x 104	Y	Y
2	14	Connemara	FE	Right retrobulbar mass	T, RB, MM, HY, TMJ	11	120.4	80 x 33	Y	Y
3	10	ISH	FE	Soft tissue mass left TMJ	TMJ, MR	3	127.2	37 x 32	Y	N
4	24	TB	FE	Unilateral left nasal discharge	PSG, LX, EA, MR	8	97.7	79 x 47	Y	N
5	8	Connemara	FE	Parotid soft tissue masses	PSG	4	71.8	27 x 35	Y	N
6	15	Irish Draft	MN	Dysphagia and weight loss	T, GP, C1, MR, HY, EA, PSG	19	109.4	83 x 57	Y	Y
7	11	ISH	MN	Dysphagia and quidding	TMJ, MM	3	90.8	37 x 18	Y	N
8	11	ISH	FE	Soft tissue masses PSG	GP, PSG, LX, C1	10	107	32 x 26	N	Y
9	16	Arabian Cross	FE	Retropharyngeal swelling and persistent neck extension	LX, C1, PSG, HY, GP	26	117	42 x 26	Y	Y
10	6	ISH	MN	Parotid region masses	TMJ, GP, PSG	19	103	20 x 20	N	Y
11	14	ISH	FE	Parotid mass lesion and around the base of the ears	GP, C1, TMJ, LX, EA, PX, PSG	60	124.5	73 x 52	Y	Y
12	8	Irish Draft	FE	Parotid mass lesions identified at PPE	PSG	3	95	19 x 11	Y	N
13	18	ISH	MN	Parotid soft tissue masses and behavioral changes	PSG, TMJ, EA, MR	18	100.5	52 x 36	Y	Y

Abbreviations: Y/N; Yes/No, FE; female entire, MN; male neutered, TB; Thoroughbred, ISH; Irish Sports Horse, HU; Hounsfield Unit, PX; Pharynx, LX; Larynx, GP; Guttural Pouches, EA; Base of ears, TMJ; Temporomandibular joint, T; Tongue, RB; Retrobulbar space, MM; Masseter muscle, HY; Surrounding the hyoid apparatus, MR; Medial to the mandibular ramus, PSG; Parotid salivary gland region, C1; Surrounding the first cervical vertebra, PPE; Pre-purchase examination

411 **Figure Legends**

412 Figure 1: Transverse CT images displayed on a soft tissue WW/WL obtained
413 from four horses included, depicting a selection of the hyperattenuating
414 melanomas identified, with or without mineralization and/or hypoattenuating
415 foci. A; CT image at the level of the occipital bone from horse 11, B; CT image
416 from horse 1 at the level of the guttural pouches, C; CT image from horse 3 at the
417 level of the vertical ramus of the mandible, D; CT image from horse 6 at the level
418 of the cheek teeth (white * indicates lesion within the tongue).

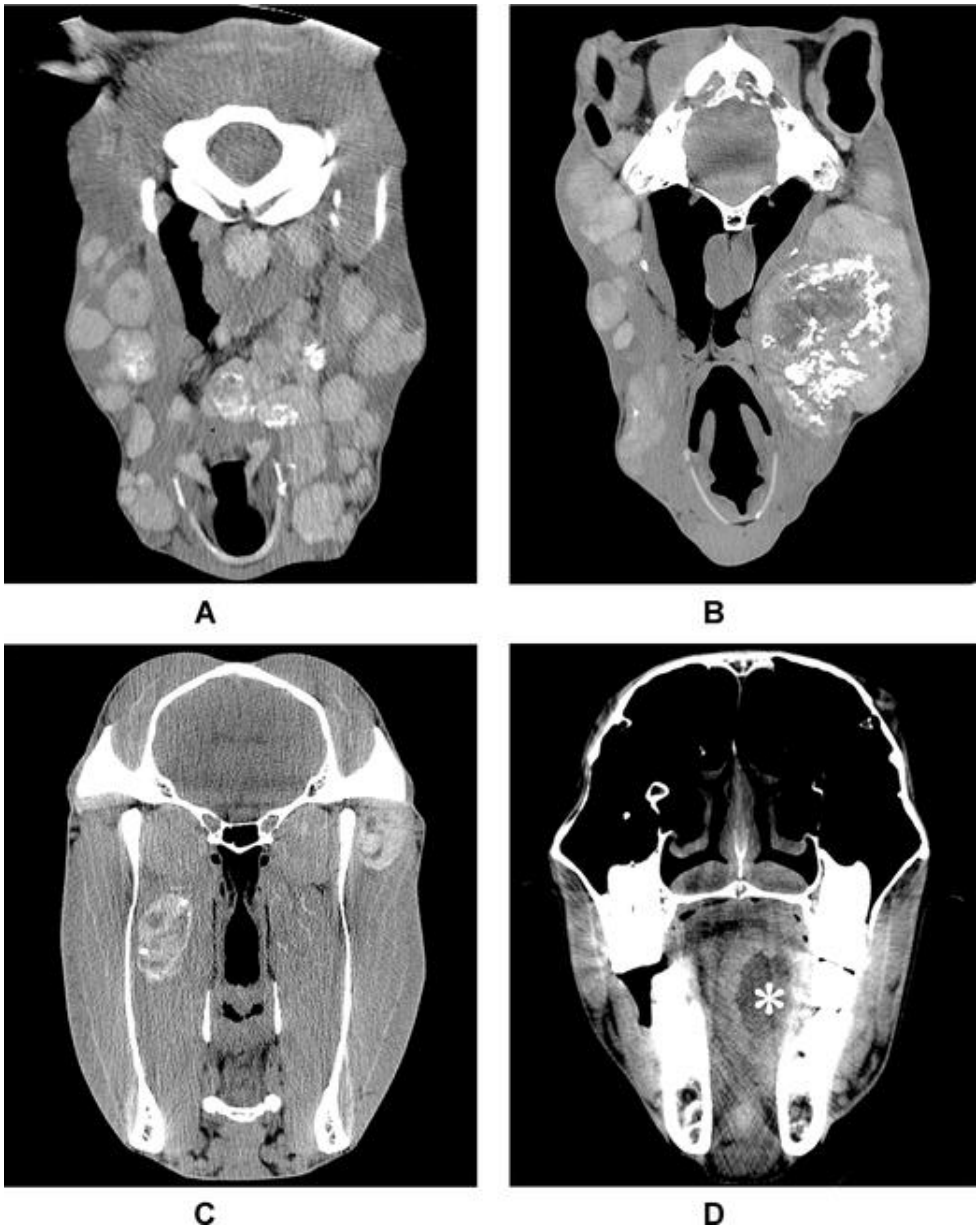

419

Figure 2: Photomicrographs of equine melanoma. A; Unbleached section stained with H&E. Note short interwoven bundles and closely packed nests of pigmented melanocytes (arrow head) interspersed with coarsely granular melanophages (large arrow). Original magnification x100. B; Bleached section stained with H&E. Note mild to moderate nuclear atypia exhibited by neoplastic melanocytes (arrow head) versus melanophages (large arrow). Original magnification x200.